Underlying Fermi surface of $Sr_{14-x}Ca_xCu_{24}O_{41}$ in two-dimensional momentum space observed by angle-resolved photoemission spectroscopy

T. Yoshida,[1] X. J. Zhou,[2] Z. Hussain,[3] Z.-X. Shen,[4] A. Fujimori,[1] H. Eisaki,[5] and S. Uchida[1]
[1]*Department of Physics, University of Tokyo, Bunkyo-ku, Tokyo 113-0033, Japan*
[2]*National Laboratory for Superconductivity, Beijing National Laboratory for Condensed Matter Physics, Institute of Physics, Chinese Academy of Sciences, Beijing 100080, China*
[3]*Advanced Light Source, Lawrence Berkeley National Laboratory, Berkeley, California 94720, USA*
[4]*Department of Applied Physics and Stanford Synchrotron Radiation Laboratory, Stanford University, Stanford, California 94305, USA*
[5]*National Institute of Advanced Industrial Science and Technology, Tsukuba 305-8568, Japan*
(Received 10 September 2008; revised manuscript received 16 June 2009; published 17 August 2009)

We have performed an angle-resolved photoemission study of the two-leg ladder system $Sr_{14-x}Ca_xCu_{24}O_{41}$ with $x=0$ and 11. "Underlying Fermi surfaces" determined from low-energy spectral-weight mapping indicates the quasi-one-dimensional nature of the electronic structure. Energy gap caused by the charge-density wave has been observed for $x=0$ and the gap tends to close with Ca substitution. The absence of a quasiparticle peak even in $x=11$ is in contrast to the two-dimensional high-T_c cuprates, implying strong carrier localization related to the hole crystallization.

DOI: 10.1103/PhysRevB.80.052504 PACS number(s): 74.25.Jb, 71.18.+y, 74.72.Dn, 79.60.−i

Since the discovery of the high-T_c superconductor in layered cuprates, one-dimensional (1D) cuprates have also attracted much interest.[1] Particularly, Cu-O ladders with an even number of coupled Cu-O chains are predicted to have a finite spin-gap reminiscent of that in the underdoped high-T_c cuprates and have the possibility of superconductivity with hole doping.[2] Ladder compounds such as $Sr_{14-x}Ca_xCu_{24}O_{41}$ (Sr14–24–41) and $LaCuO_{2.5}$ in which two-dimensional CuO_2 planes is reorganized into 1D segments have long been envisioned to bridge 1D chain systems, where Luttinger liquid behaviors are predicted, and two-dimensional (2D) plane systems, which is the stage of the high-T_c superconductivity. Sr14–24–41 is composed of alternating stacks of the plane of edge sharing CuO_2 chains, (Sr and Ca) layer, and the plane including two-leg Cu_2O_3 ladders. With Ca substitution, holes are transferred from the chain sites to the ladder sites.[3] From the optical reflectivity measurement of Sr14–24–41 at room temperature, the number of holes doped into the Cu_2O_3 ladder plane is already 0.07/Cu atom for $x=0$, which should be enough to realize superconductivity in 2D cuprate.[3] However, the $x=0$ samples are insulating and show an activated behavior in the resistivity.[4] Upon Ca substitution for Sr, holes localized in the chains are transferred to the ladders and induce mobile carriers on the ladder. When $x>11$, the mobile carriers exhibit superconductivity under high pressure.[5] To understand the electronic structure of such quasi-1D systems, angle-resolved photoemission spectroscopy (ARPES) is a powerful tool because it provides us with momentum-resolved information about the electronic states. In the previous ARPES experiments on the ladder system Sr14–24–41, two dispersive features along the ladder and chain directions were observed and assigned to the ladder-derived band (near E_F) and the chain-derived band (~1 eV below E_F), respectively.[6,7] However, in the previous results, only one-dimensional momentum dependence along the ladder/chain direction has been studied in momentum space. Since superconductivity in this system appears when application of pressure causes a dimensional crossover from one to two as reflected in electrical resistivity,[8] two-dimensional electronic structure has been thought to be crucial to the superconductivity. In the present work, we have performed ARPES experiments on the two-leg ladder compound Sr14–24–41 with $x=0$ and 11 and clarified spectral-weight distribution in the two-dimensional momentum space. The ARPES results clearly demonstrate the quasi-one-dimensional electronic structure of the ladder but with finite-energy dispersion perpendicular to the ladder direction. Also, an energy gap of the ladder band of ~70 meV observed for $x=0$ tends to close with Ca substitution. The line shape of the gapped states will be compared with those for the 2D high-T_c cuprates.

The ARPES measurements were carried out at BL10.0.1 of Advanced Light Source, using incident photons of 55.5 eV. We used a Scienta SES-200 analyzer with total-energy resolution of 20 meV and momentum resolution of $0.02\pi/c$, where $c=3.95$ Å is the Cu-O-Cu distance along the ladder direction. The lattice-constant perpendicular to the ladder within the ladder plane is $a=11.46$ Å. We studied high-quality single crystals of $Sr_{14-x}Ca_xCu_{24}O_{41}$ with $x=0$ and 11 grown by the traveling-solvent floating-zone method. Measurements were performed in an ultrahigh vacuum of 10^{-11} Torr. The samples were cleaved *in situ* and measured at 20 and 150 K for the $x=11$ and 0 samples, respectively. In the present measurements, the electric field vector **E** of the incident photons lie in the ladder and chain plane.

Figure 1 shows spectral intensity in energy-momentum (E-k) space along the ladder (k_z) direction and corresponding energy-distribution curves (EDCs) for these k_x values. Dots in the E-k maps are the peak position of the momentum-distribution curves (MDCs). Here, MDCs reflect energy dispersion of the "quasiparticle" (QP) although the MDC width is very broad. In panels (a4) and (b4), a broad structure around −1 eV below the Fermi level (E_F) is assigned to energy bands from the chain states according to the previous studies.[6,7] On the other hand, the structure around −0.5 eV at $k_z \sim 0.5$ can be ascribed to the ladder electronic structure since the dispersion at $|k_z| < 0.5$ correspond well to that pre-

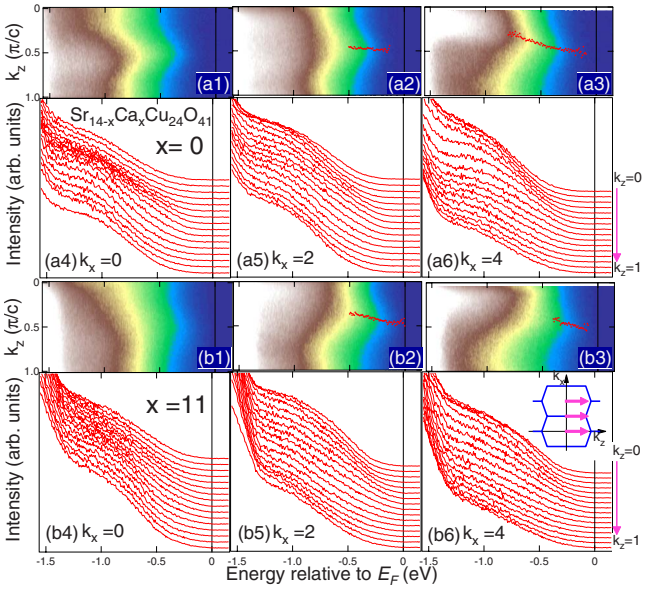

FIG. 1. (Color online) ARPES spectra for $Sr_{14-x}Ca_xCu_{24}O_{41}$ ($x=0,11$). Panels (a1)–(a3) and (b1)–(b3) show spectral intensities in energy-momentum (E-k) space along the k_z direction for $k_x(\pi/a)=0$, 2, and 4. Dots are the peak position of the MDCs. Panels (a4)–(a6) and (b4)–(b6) show EDCs corresponding to the E-k intensity map in (a1)–(a3) and (b1)–(b3), respectively. Inset for panel (b6) illustrates corresponding cuts in momentum space and the ladder Brillouin zone.

dicted by band-structure calculation.[9] This structure shows clear dispersion and have a bottom of the band around $k_z=0$ as shown in panels (a6) and (b6). Although MDCs show the remnant of a dispersive band, a sharp quasiparticle peak in the EDCs was not observed even for the $x=11$ sample. The intensity of the ladder component is enhanced in the second Brillouin zone (BZ) [Figs. 1(a6) and 1(b6)] while that of the chain band is suppressed. Since the ladder can be regarded as a portion of the CuO_2 plane, the enhancement of the ladder spectra in the second BZ may be caused by similar matrix-element effects as seen in the high-T_c cuprates. The spectral intensities of the chain bands are enhanced in the first BZ [panels (a4) and (b4)] while those in the second BZ is strongly suppressed [panels (a6) and (b6)]. These contrasted behaviors of the spectral intensity between the ladder and the chain bands manifest the difference in the orbital symmetry of the wave functions since the Cu $3d_{xy}$ orbitals for the chain band are rotated by 45° from the Cu $3d_{x^2-y^2}$ orbitals for the ladder band.

Spectral weight at various binding energies are mapped in momentum space in Fig. 2. From comparison between $x=0$ and 11, the low-energy spectral weight for $x=11$ is more intense than that in $x=0$ [Figs. 2(a2) and 2(b2)]. Particularly, the map at E_F for $x=0$ shows almost no intensity, indicating that the energy gap is opened on the entire "Fermi surface." Note that spectral-weight distribution in the insulating parent compounds of high-T_c cuprates resembles the original noninteracting Fermi surface, i.e., shows remnant Fermi surf-

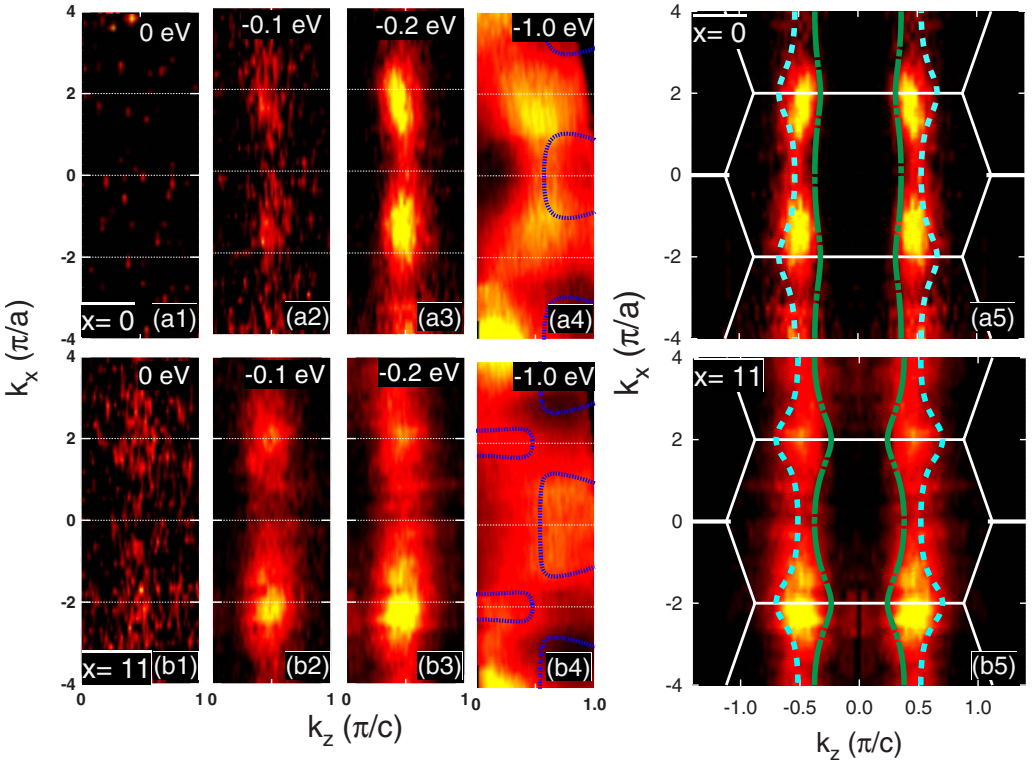

FIG. 2. (Color online) Spectral-weight mapping of the ARPES spectra of $Sr_{14-x}Ca_xCu_{24}O_{41}$ ($x=0,11$). Panels (a1)–(a4) and (b1)–(b4) show the intensity map for $x=0$ and 11 at each energy from the E_F, respectively. Dotted lines in panels (a4) and (b4) indicate the Fermi surfaces of the chain band predicted by band-structure calculation (Ref. 9). Panels (a5) and (b5) are intensity maps for −0.2 eV symmetrized with respect to the $k_z=0$ line and represent the "underlying Fermi surfaces." Dashed and dash-dotted lines indicate Fermi surfaces of the bonding and antibonding bands of the ladder predicted by the band-structure calculation (Ref. 9).

aces.[10] While the low energy spectra represent the quasi-one-dimensional Fermi-surface shape of the electronic structure of the ladder, in the high-energy range ~ -1 eV [Figs. 2(a4) and 2(b4)], the spectral weight distribution is more widely distributed in momentum space and is more strongly k_y dependent, i.e., two dimensional. These structures come from the chain states and are similar to the Fermi surface of chain state predicted by the band-structure calculation[9] as superimposed on the mapping in panels (a4) and (b4). However, note that the chain states is not observed near the Fermi level but observed in the high-energy range ~ 1 eV since the holes in the chain is strongly localized unlike those in the ladders.

In Figs. 2(a5) and 2(b5), the observed spectral weight at the energy of -0.2 eV are symmetrized with respect to the $k_z=0$ line in two-dimensional momentum space. One can see that the spectral-weight distribution is approximately confined between the bonding and antibonding Fermi surfaces predicted by the band calculation.[9] Furthermore, the intensity around the zone boundary is enhanced in both samples. The observed intensity modulation along the k_y direction indicates finite interladder hopping integrals, which cause the bonding and antibonding band splitting, although the EDCs are too broad to separate the bonding and antibonding bands. The spectral intensity of $x=0$ in the first BZ is stronger than those in the second BZ while $x=11$ shows the opposite behavior. This difference may come from the intensity of the chain structure in the high-energy region. As shown in Figs. 1(a4) and 1(b4), the chain structure in $x=0$ is clearer than that in $x=11$. The observed change in the spectral-weight distribution by Ca substitution indicate spectral-weight transfer from the high energy to the low energy in the ladder electronic states, which is related to the hole transfer from the chain to the ladder.[3]

We have estimated the energy gap near E_F from the integration of ARPES spectra on a cut along the k_z direction as shown in Fig. 3. As shown in Figs. 3(a) and 3(b), the energy-gap size for $x=0$ can be estimated as $\Delta \sim 70$ meV, consistent with the result of the optical conductivity, $2\Delta \sim 130$ meV. The optical gap is interpreted as a charge-density wave (CDW) gap.[11] For the $x=11$ sample, although the slope of the spectra reach E_F, no clear Fermi edge is observed. Also, the integrated MDC spectra for $k_x=2$ is slightly closer to the E_F than that in $k_x=4$ while there is almost no difference between them for $x=0$. This can be taken as a signature of the increased two dimensionality in $x=11$. However, the change in $x=11$ is still small and far from a two-dimensional electronic structure. The transport properties in the ladder direction of $x=11$ show metallic behavior ($d\rho/dT>0$) (Ref. 8) and a Drude peak in the optical conductivity[3] at high temperatures. However, the electrical resistivity shows localization behavior at low temperatures and the Drude peak has a suppression in the low energy (~ 10 meV) region. Therefore, we conclude that the broad spectral line shape without clear Fermi edge reflects the localization at low temperatures seen in the transport properties.

The absence of QP is contrasted with the case of the lightly doped high-T_c cuprates, which shows clear a QP in the nodal direction, although the hole concentration ~ 0.2 of the ladder for the $x=11$ sample is almost the same as that for the overdoped cuprates.[3] Note that the present data do not show clear indications of surface states caused by off stoichiometry[12] nor replica from surface reconstruction.[13] In order to compare the present results with the high-T_c cuprates in Figs. 3(c) and 3(d), we show integrated ARPES spectra of $La_{2-x}Sr_xCuO_4$ (LSCO) (Refs. 14 and 15) along the $(\pi,0)-(\pi,\pi)$ and $(0,0)-(\pi,\pi)$ directions, respectively. In LSCO, because of the pseudogap around $(\pi,0)$, the intensity decrease with approaching E_F. Particularly, the spectral line shape of $x=0.03$ is similar to the ladder spectra for $x=11$ shown in Fig. 3(b). Since the shape of the Fermi surface around $(\pi,0)$ in the underdoped 2D cuprates is a quasi-one dimensional,[16] this similarity in the spectral line shape implies that the mechanism of the pseudogap formation is similar between the ladder and the 2D cuprates. On the other hand, the clear Fermi edge indicating the E_F crossing of QP in the nodal region of LSCO [Fig. 3(d)] is contrasted with the case of the ladder, probably reflecting the difference between the 1D and 2D electronic structures. This 1D-2D difference would be related to the facts that two dimensionality makes hole carriers mobile and that three-leg ladder compounds can easily become metallic with hole doping compared to the two-leg ladder system. In a two-leg ladder, Zhang-Rice singlet has a strong tendency toward hole crystallization as observed in the x-ray scattering even in $x=11$ samples.[17]

Finally, let us discuss the condition for the occurrence of

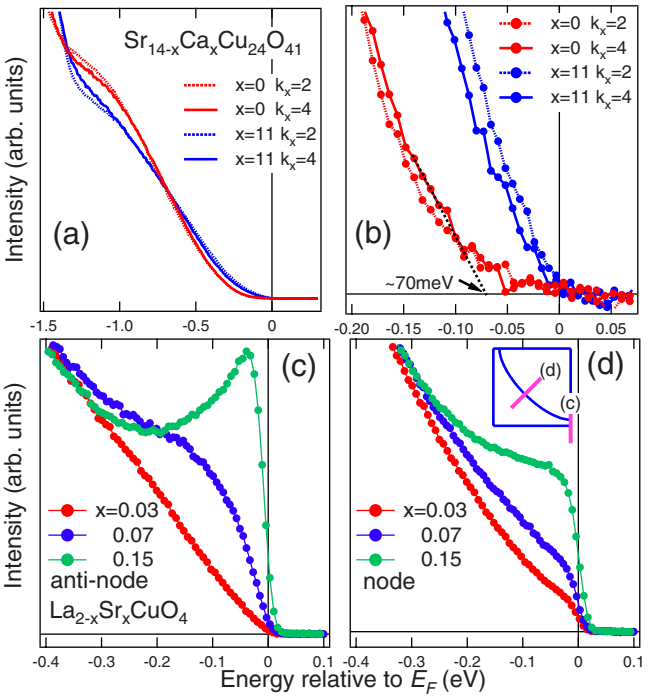

FIG. 3. (Color online) Integrated intensities of MDC as a function of energy for $Sr_{14-x}Ca_xCu_{24}O_{41}$. (a) Integrated spectra along the k_z-axis direction. Panel (b) is an enlarged plot of panel (a). A Gap size for $x=0$ is obtained as illustrated by a black dotted line. Panels (c) and (d) show integrated ARPES spectra of two-dimensional high-T_c cuprates $La_{2-x}Sr_xCuO_4$ along $(\pi,0)-(\pi,\pi)$ and the $(0,0)-(\pi,\pi)$ directions, respectively, (see inset) for comparison with the present results. Note that the hole doping level of the ladder is ~ 0.07 for $x=0$ and ~ 0.2 for $x=11$ (Ref. 3).

superconductivity in the ladder compounds. We have found that the electronic structure is still quasi-one dimensional even in $x=11$ samples. On the other hand, when the superconductivity occurs under high pressure, the transport properties become rather two dimensional, i.e., anisotropy of the a- and c-axis resistivities become small.[8] As for the electronic structure, the relatively isotropic-transport properties may be a result of a topological change in the Fermi surface from one dimension to two dimension. The shift of the chemical potential caused by the hole transfer from the chain to the ladder under high pressure may cause a two-dimensional Fermi surface of the ladder bands. Therefore, two-dimensional electronic structure may be necessary to the superconductivity analogous to the two-dimensional high-T_c cuprates.

In summary, we have performed an ARPES study of the two-leg ladder system Sr14–24–41 to investigate the Ca substitution effects on the two-dimensional electronic structure. The intensity modulation due to interladder hopping has been observed, indicating finite 2D effect. The CDW gap size for $x=0$ is about 70 meV and reduced to 10–20 meV for $x=11$, consistent with the results of the optical conductivity.[11] We did not, however, observe a clear QP peak even in the metallic $x=11$ samples. This behavior is contrasted with that of the lightly doped LSCO, which shows a clear QP peak crossing E_F in the nodal direction. Possible origins of the absence of a QP are attributed to the strong localization of doped holes due to the quasi-one dimensionality.

This work was supported by a Grant-in-Aid for Scientific Research in Priority Area "Invention of Anomalous Quantum Materials," a Grant-in-Aid for Young Scientists from the Ministry of Education, Science, Culture, Sports and Technology, and the U.S. D.O.E. under Contracts No. DE-FG03-01ER45876 and No. DE-AC03-76SF00098. ALS is operated by the Department of Energy's Office of Basic Energy Science, Division of Materials Science.

[1] E. Dagotto, Rep. Prog. Phys. **62**, 1525 (1999).
[2] E. Dagotto, J. Riera, and D. Scalapino, Phys. Rev. B **45**, 5744 (1992).
[3] T. Osafune, N. Motoyama, H. Eisaki, and S. Uchida, Phys. Rev. Lett. **78**, 1980 (1997).
[4] N. Motoyama, T. Osafune, T. Kakeshita, H. Eisaki, and S. Uchida, Phys. Rev. B **55**, R3386 (1997).
[5] M. Uehara, T. Nagata, J. Akimitsu, H. Takahashi, N. Mori, and K. Kinoshita, J. Phys. Soc. Jpn. **65**, 2764 (1996).
[6] T. Takahashi, T. Yokoya, A. Ashihara, O. Akaki, H. Fujisawa, A. Chainani, M. Uehara, T. Nagata, J. Akimitsu, and H. Tsunetsugu, Phys. Rev. B **56**, 7870 (1997).
[7] T. Sato, T. Yokoya, T. Takahashi, M. Uehara, T. Nagata, J. Goto, and J. Akimitsu, J. Phys. Chem. Solids **59**, 1912 (1998).
[8] T. Nagata, M. Uehara, J. Goto, J. Akimitsu, N. Motoyama, H. Eisaki, S. Uchida, H. Takahashi, T. Nakanishi, and N. Môri, Phys. Rev. Lett. **81**, 1090 (1998).
[9] M. Arai and H. Tsunetsugu, Phys. Rev. B **56**, R4305 (1997).
[10] F. Ronning, C. Kim, D. L. Feng, D. S. Marshall, A. G. Loeser, L. L. Miller, J. N. Eckstein, I. Bozovic, and Z.-X. Shen, Science **282**, 2067 (1998).
[11] T. Vuletić, B. Korin-Hamzić, S. Tomić, B. Gorshunov, P. Haas, T. Room, M. Dressel, J. Akimitsu, T. Sasaki, and T. Nagata, Phys. Rev. Lett. **90**, 257002 (2003).
[12] D. Pillay, M. D. Johannes, and I. I. Mazin, Phys. Rev. Lett. **101**, 246808 (2008).
[13] A. Damascelli, K. M. Shen, D. H. Lu, and Z.-X. Shen, Phys. Rev. Lett. **87**, 239702 (2001).
[14] T. Yoshida, X. J. Zhou, K. Tanaka, W. L. Yang, Z. Hussain, Z.-X. Shen, A. Fujimori, S. Sahrakorpi, M. Lindroos, R. S. Markiewicz, A. Bansil, S. Komiya, Y. Ando, H. Eisaki, T. Kakeshita, and S. Uchida, Phys. Rev. B **74**, 224510 (2006).
[15] T. Yoshida, X. J. Zhou, D. H. Lu, S. Komiya, Y. Ando, H. Eisaki, T. Kakeshita, S. Uchida, Z. Hussain, Z.-X. Shen, and A. Fujimori, J. Phys.: Condens. Matter **19**, 125209 (2007).
[16] X. J. Zhou, T. Yoshida, S. A. Kellar, P. V. Bogdanov, E. D. Lu, A. Lanzara, M. Nakamura, T. Noda, T. Kakeshita, H. Eisaki, S. Uchida, A. Fujimori, Z. Hussain, and Z.-X. Shen, Phys. Rev. Lett. **86**, 5578 (2001).
[17] P. Abbamonte, G. Blumberg, A. Rusydi, A. Gozar, P. G. Evans, T. Siegrist, L. Venema, H. Eisaki, E. D. Isaacs, and G. A. Sawatzky, Nature (London) **431**, 1078 (2004).